Int. j. adv. multidisc. res. stud. 2023; 3(3):703-708

Received: 21-04-2023
Accepted: 01-06-2023

International Journal of Advanced Multidisciplinary Research and Studies

ISSN: 2583-049X

Biological and Medical Efficacy of Zinc Oxide Nanoparticles Manufactured Using *Saccharomyces boulardii* against Burkholderia sp. Isolated from Diabetic Foot Patients

[1] Hussein Ali Abdulradha, [2] Suaad Waheed Alhadrawi
[1, 2] Department of Biology, Faculty of Science, University of Kufa, Iraq

Corresponding Author: **Hussein Ali abdulradha**

Abstract
The aim of the present study is to manufacture zinc nanoparticles using the probiotic Saccharomyces boulardii and to evaluate their biological activity. The biological approach of synthesizing nanoparticles is becoming more and more important since it is more practical and ecologically friendly than chemical and physical methods of production.
Methods: Zinc acetate was added at a dose necessary to biosynthesize ZnO NPs from S. boulardii's cellfree supernatant (1 mM).
Results: The resulting mixture's color changed from light to dark after 150 rpm of incubation, and the antibacterial activity provided confirmation that S. bularedii was in charge of this change in appearance. Atomic force microscopy (AFM), scanning electron microscopy (SEM), energy dispersive spectroscopy (EDS), ultraviolet-visible spectroscopy (UVS), and X-ray diffraction (XRD) all played a part in the characterization (AFM). UV-visible spectroscopy was used to measure the ZnO NPs' spectra, which were found to be (34***1***.75 nm) in the reaction mixture. ZnO NPs had a crystal size of ***29***.1 nm, according to the XRD. A SEM showing the consistent, spherical shape and average size (24.61 nm) was made available. ZnO NPs in their elemental form were examined using EDS. ZnO NPs had an average diameter of (62.89 nm) and a three-dimensional structure that could be seen using AFM.The FTIR spectrum reveals a variety of functional groups that are present at various locations.Specifically, B. cepacia bacteria were identified from diabetic foot ulcers. When the produced nanoparticles were tested against the pathogenic culture of this bacteria, a very good zone of inhibition was observed.

Keywords: Medical, Zinc Oxide, Nanoparticles, Diabetic Foot

Introduction
Diabetic foot infections (DFIs) is the problem frequent, complicated, and expensive.a significant clinical and economical burden on diabetic individuals (Veve *et al*., 2022) [28]. One of the most terrifying diabetes consequences. Diabetic foot ulcers (DFU) is a significant case for diabetes people because majority of them visit hospitals for it. Trauma that is either direct or indirect might result in DFU. Once DFU has developed, the wound will become injured, suffer from loss of sensation, peripheral artery disease, and possibly even start to necrotize cells, leading to the eventual amputation of the infected foot (Hicks, C. W *et al*., 2016) [13]. Diabetic foot ulcers cause over 80% of all lower limb amputations (Pecoraro *et al*, 1990). According to (Singh, *et al*. 2005) [26], individuals with diabetes have a 25% higher risk of losing a limb than those without the disease. A non-pathogenic yeast called Saccharomyces boulardii has been used for many years as a probiotic agent to prevent or treat a number of gastrointestinal problems in humans, including antibiotic-associated diarrhea (Dahiya & Nigam, 2022) [6]. In order to manufacture nano-sized particles with specific functions, nanobiotechnology combines biological concepts with physical and chemical processes. It offers a practical substitute for expensive chemical and physical methods of producing nanoparticles. Based on fundamental qualities including scale, distribution, and shape, nanoparticles have new or changed properties. There are a growing number of innovative uses for NPs and nanomaterials (Begum *et al*., 2022) [2]. Zinc oxide nanoparticles (ZnO NPs) have drawn significant attention due to their numerous uses in biotechnology and bioengineering as antibacterial, antifungal, antioxidant, and biofilm prevention agents (Zhang *et al*., 2022) [31].
Burkholderia cepacia is detection as a group of highly virulent organisms known as the Burkholderia cepacia Complex (Bcc). Bcc is ubiquitous in nature and is most commonly found in moist environments, plant roots and soils. Due to its high inherent antibiotic resistance, Bcc is a major cause of morbidity and mortality in inpatients. It is most commonly reported in immune compromised patients, especially those with cystic fibrosis (Ranjan, *et al*., 2017) [22]. B. cepacia is a rod-shaped, motile,

catalase-positive, Gram-negative, non-spore-forming, and lactose-non-fermenting bacteria (Tavares, *et al*., 2020). They are regarded as a typical environmental species that have been isolated as free-living microorganisms, and they coexist closely with several animals, plants, ameobozoon hosts, and fungi (Stopnisek, *et al*., 2016; Xu, *et al*., 2016) [27, 29]. Like many opportunistic pathogens, B. cepacia can establish an infection in any favorable environment.

Experimental

Preparation supernatant of *S. boulardii*

Saccharomyces boulardii was carefully selected from a variety of yeast species based on its resistance to industrial ZnO NPs and its capacity to produce ZnO NPs extracellularly (in the supernatant). S. boulardii was injected into Sabouraud dextrose broth (SDB), which was then incubated for 24 hours at 37°C. For 25 minutes at 4°C and 6000 rpm, the culture was centrifuged to separate the S. boulardii supernatant. It was decided to create cell-free supernatants for the production of zinc oxide nanoparticles. (Mohd Yusof *et al* 2020) [18].

Biosynthesis of ZnO NPs Using Cell Free Supernatant

S. boulardii used zinc acetate as the precursor for the production of ZnO NPs. To the cell-free supernatant,zinc acetate was added at a concentration of 1 mM and stirred. The resulting solutions were incubated for 24 hours at 37° C in a shaking incubator at 150 rpm. After incubation, the reaction mixture was centrifuged at 6000 rpm for 25 min. at 4°C to remove the supernatant. The supernatant was then replaced with deionized distill water, and the centrifugation process was repeated three more times under the same conditions to remove any remaining supernatant.The pellet-shaped collection of nanoparticles was then dried in an oven at 40°C for 18 to 24 hours. The dry powder was carefully gathered and kept in storage for additional investigation. (Ramesh *et al* 2021) [21].

Characterization of ZnO Nanoparticles

Visible UV ZnO NPs were characterized using X-ray diffraction and spectroscopy. In the electron microscopy unit, SEM was utilized to characterize the morphology of nanoparticles. The microscope functioned with variable magnifications, low vacuum, a spot size of 4, and working distances of 5-10 mm at an accelerated voltage of 15 KV (Shafaghat, 2015) [24]. Utilizing Bruker EDS coupled with SEM, elemental analysis of a single particle was performed. EDS was utilized to do a point analysis with an accelerating voltage of 10 KV, a spot size of 5, and working distances of 10 mm (Shirley & Jarochowska, 2022) [25]. The ZnO NPs were characterized using AFM. The FTIR spectrophotometer was used to measure the synthesized formulations transmittance.

Antibacterial Activity of ZnO Nanoparticles

Biogenic ZnO NPs' antibacterial activity was delivered by agar well diffusion against several pathogenic, multi-drug resistant gram positive and gram-negative bacteria isolated from diabetic foot infections. Each tested bacterium was suspended to the McFarland standard (0.5N) and then swabbed individually onto sterile Muller-Hinton Agar (MHA) plates. Agar was pierced with a 7 mm sterilized cork borer, and 100 l of biogenic ZnO NPs were added to each well at various concentrations (100, 200, and 300 g/ml), which were then incubated for 24 hours at 37 °C. The inhibitory zones were then quantified. (Rajeshkumar and Malarkodi, 2014) [20]. Antioxidant activity of biogeneic zinc oxide nanoparticles *in vitro*. We tested the extracts' capacity to scavenge free radicals using the DPPH (2, 2-diphenyl-1-picrylhydrazyl) method. Methanol was used to create the DPPH solution (0.006% w/v). Employing a 96-well plate, 200 µL of freshly made DPPH solution was put in the control well, and 200 µL of methanol was put in the blank well. 100 µL of (ZnO) NPs (1,0.5, 0.25, 0.12)mg/ml were then added to each well of the DPPH solution, bringing the total volume to 200 µL. Discoloration was measured at 517 nm after 30 min. of dark incubation. As a control, DPPH solution was employed. The following equation was used to compute the percentage of DPPH free radical scavenging:

DPPH Scavenging Impact (%) = (Ao –A1) / Ao × 100

Where (A1) was the absorbance in the presence of the ZnO NPs and (Ao) was the absorbance in the control (Goyal *et al*., 2010) [12].

Hemolysis Effect of (ZnO) NPs

The percentage of hemolysis was used to determine the (ZnO) NPs' hemolytic toxicity. A healthy, unmedicated human donor's blood was drawn and collected in the anticoagulant EDTA. One healthy donor's blood was used for the hemolysis experiments, which involved adding 15 µL of nanoparticles (ZnO)NPs in various concentrations (1,0.5, 0.25, and 0.12 mg, suspended in tyrode), tyrode as a negative control, or triton (X-100) as a positive control to 285 L of whole blood. The suspension is incubated on a shaking plate for 4 hours at room temperature. The suspension is centrifuged at 10000 g for 5 minutes after the incubation period. Using a microplate scanning spectrophotometer, the supernatant is read in a 96-well plate at 550 nm (Laloy *et al*., 2014) [16]. The formula used to determine the % hemolysis was:

H (%) = (sample-tyrode)/(Triton X-100) (1)%-tyrode) x 100

Results and Discussion

Biosynthesis of zinc oxide nanoparticles the extracellular production of ZnO NPs by Saccharomyces boulardii was demonstrated utilizing cell free supernatant and zinc acetate (1Mm) as a precursor. The free cell supernatant of S. boulardii is able to alter the color of the reaction mixture after being incubated for 24 hours at 37°C and 150 rpm while being shaken, which serves as an indication for the biosynthesis of ZnO NPs. The microbial cell secretes reductases that are used in the bio reduction of metal ions into the appropriate NPs during the extracellular creation of nanoparticales (Ovais *et al*., 2018). The antibacterial behavior and the reaction mixture's color change from light to dark after 150 rpm incubation provided as evidence that S. bularedii was responsible for the ZnO NPs' production. In contrast to the cell, where the components in the cytoplasm would strive to maintain a steady environment and call for more purification, the environment of the culture supernatant may be simply improved. Therefore, rather of using cells themselves, supernatant may be utilized to make zinc oxid nanoparticles (Bahrulolum *et al*, 2021). Numerous investigations have suggested that the creation of metal nanoparticles involves NADH and NADH-dependent enzymes. It appears that the reduction was initiated by the

NADH-dependent reductase acting as an electron transporter to transfer electrons from the NADH (Ranganath *et al*., 2012; Joerger *et al*., 2000). The morphology depends on a number of chemical and physical factors, including incubation period, pH, the makeup of the culture media and whether the organism grows in the light or the dark. (Durán *et al*., 2011) [11].

UV-Visible Spectroscopy

When ZnO NPs were analyzed using UV-vis spectrophotometry,an absorption peak at 34***1.6*** nm wavelength was seen, showing that ZnO NPs were present in the reaction solution. Fig 1. Visual inspection and UV-vis spectroscopy measurements of the surface plasmon resonance (SPR) band can both attest to the biogenesis of nanoparticles. Nanoparticles' single SPR band demonstrates their spherical form. (Abdulhassan, 2016) [1].

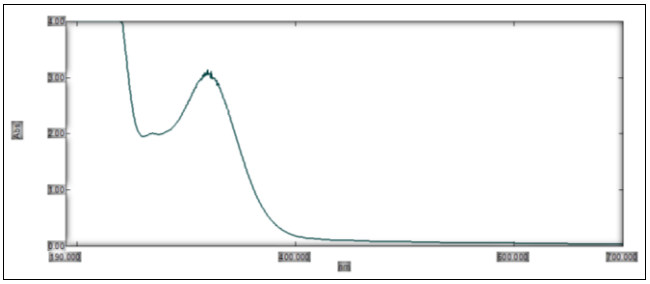

Fig 1: UV-visible spectroscopy analysis of ZINC NPs synthesis by *S. bularedii*

XRD Analysis of Nanoparticles

S. boulardii formed ZnO NPs with average crystal sizes of ***29.1*** nm, according to the XRD, Fig 2. Intense peaks at 2 corresponding to about the lattice plane indices were seen in the X-ray diffraction pattern of ZnO NPs produced extracellularly by S. boulardii Their crystalline structure is shown by the peaks' sharpness in the XRD spectrum (Yallappa *et al* 2013) [30]. The ZnO NPs biosynthesized from S. boulardii were ***29.1*** nm in size, which is different from the typical size ranges shown in (Loganathan, *et al*., 2021) [17] by 64.74 nm.

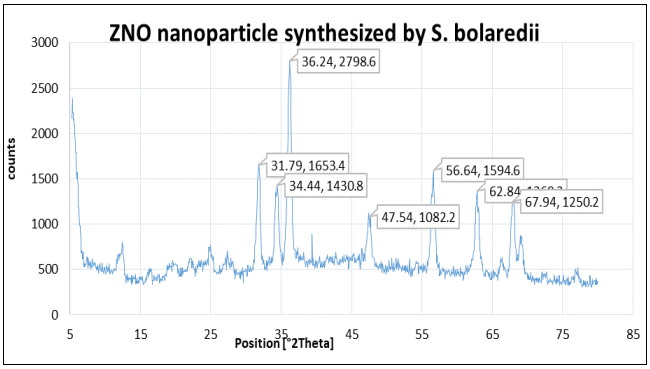

Fig 2: XRD analysis the size of Biosynthesized Zno nanoparticles S. bularedii

SEM Analysis of ZnO NPs

The SEM findings revealed well-dispersed nanoparticles and homogeneous ZnO NPs with an average size of 24.61 nm and spherical shape (see Fig 3). In accordance with the findings of Dobrucka & Dugaszewska, biogenic ZnO NPs were agglomerated with a spherical shape using the SEM to define the shape and size of the nanoparticles.

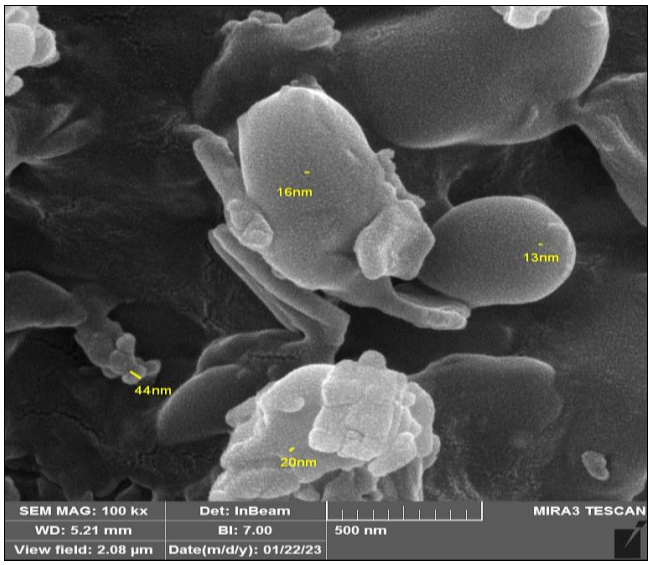

Fig 3: SEM Micrograph of biogenic Znic nanoparticle synthesized by S. bolaredii

EDS Analysis of Nanoparticles

The presence of elemental zinc oxide indicated that S. boulardii supernatant had reduced the zinc ions in the mixture. Strong signals from the Zn atoms, medium signals from oxygen, and weaker signals from other elements were seen in the EDS spectrum that was captured in point and map mode. Zn had an elemental component weight percentage of 30.8% and an oxygen content of 69.2% (Fig 4, Table 1). The incident ZnO NPs were measured using (EDS) analysis by looking at the optical absorption peaks of the zinc oxide components. The presence of elemental zinc demonstrated that ions were reduced throughout themicroorganism's response. Strong signals from the NPs atoms were seen in the EDS spectra when it was captured in spot-profile mode, compared to medium signals from oxygen and weaker signals from other atoms. The outcome was comparable with (Caroling *et al* 2013) [4].

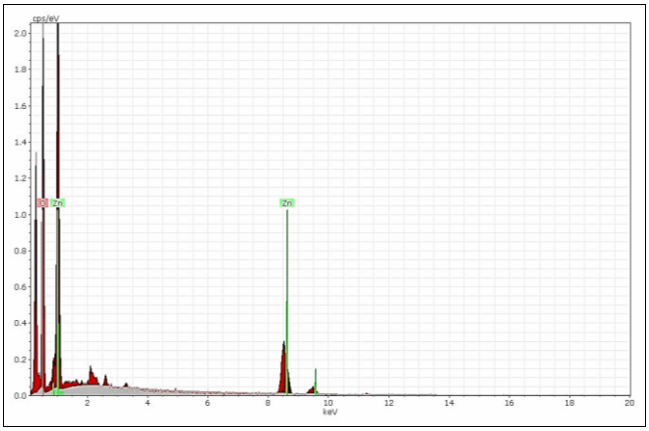

Fig 4: EDS analysis of Zinc NPs synthesis by S.bularedii

Table 1: Elemental analysis of Zinc NPs synthesis by by S.bularedii

Spectrum: Acquisition

Element	Series	unn. C [wt.%]	norm. C [wt.%]	Atom. C [at.%]	Error (1 Sigma) [wt.%]
Oxygen	K-series	34.07	69.20	90.18	5.76
Zinc	K-series	15.16	30.80	9.82	0.78
	Total:	49.23	100.00	100.00	

AFM Analysis of Nanoparticles

S. boulardii generated ZnO NPs with an average diameter of 94.9 nm and an average roughness of 8.9 nm, according to atomic force microscope (AFM) examination (Fig 5, 6). ZnO NPs' three-dimensional forms were revealed by AFM examination, and the average diameter of ZnO NPs derived from S. boulardii was 62.89 nm. This result may be attributed to differences in the bio-reduction that may be return to the qualitative and quantitative of extracellular protein/enzyme and other biomolecules that offered in the culture of each microorganism, in addition to their ability of interaction with precursor for synthesized (Zinc acetate). Nanoparticles amalgamation was better in terms of quality; minimum size and less polydispersity, with S. bularedii (Chaudhari, *et al* 2012) [5].

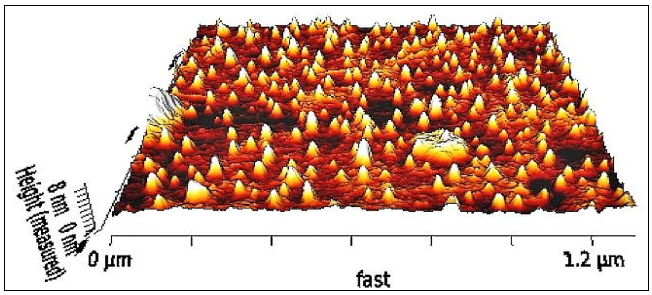

Fig 5: AFM analysis shows three-dimension image, and topography of biogenic ZnO NPs synthesis by *S. bularedii*

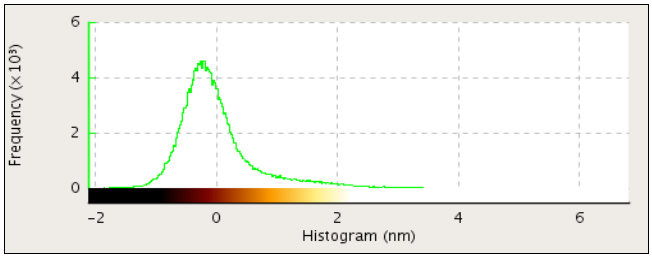

Fig 6: Granularity and accumulation distribution chart of biogenic ZnO NPs synthesis by *S. bularedii*

Fourier Transform Infrared Spectroscopy (FTIR) Analysis of Nanoparticles

The FTIR spectrum displays distinct functional groups at various places; the wavenumber ranges from 400 cm-1 to 4000 cm-1, and the peak areas below and above 1500 cm-1 are referred to as the fingerprinting region and diagnostic region, respectively (Onyszko *et al* 2022) [19]. Fig 7 shows the diagnostic area for the ZnO NPs produced by S. bularedii, which includes broad band peaks at 3448 cm-1 for O-H stretching, 2923 cm-1 for C-H stretching vibration of alkane groups, 2343 cm-1 for C-C stretching, and 1637 cm-1 for C-C stretching (alkene). These findings are consistent with (Kaschner *et al* 2002) [15].

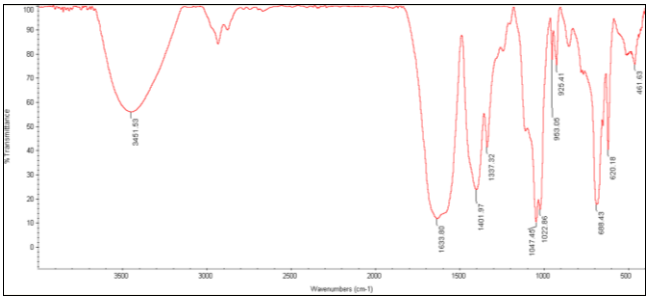

Fig 7: Fourier-transform infrared spectroscopy (FTIR) spectra of ZnO NPs synthesized by S. bularedii

Antibacterial Activity

In this work, which comprised the biosynthesis of zinc oxide nanoparticles and evaluation of their efficiency against pathogenic bacteria isolated from diabetic foot ulcers, and by three bis of all the isolation obtained the agar well diffusion method was used for detecting the antibacterial activity of biogenic NPs. ZnO NPs with different concentrations (300, 200; 100)µg/ml. Zno, produced by S. bularedii displayed the maximum inhibitory area (19 mm), at a concentration of 300 in isolation No. 7, and the lowest inhibition area (11 mm). Show Table 2 and Fig 8.

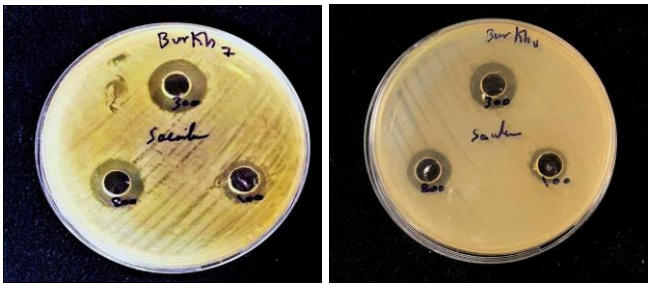

Fig 8: The agar well diffusion method was used for detecting the antibacterial activity of biogenic NPs.ZnO NPs with different concentrations (300, 200; 100)µg/ml

These results are in accordance with (Dobrucka & Dugaszewska 2016) [10]. The investigation also revealed (P 0.05), Table significant differences between the various concentrations (3). ZnO nanoparticles, according to (Divya *et al* 2013) [8], damage bacterial membranes most likely by producing reactive oxygen species including superoxide and hydroxyl radicals. This is dependent on the type of surface that certain bacteria have. Additionally, according to reports, the antibacterial activity is influenced by the kind of surfactant utilized as well as the ZnO nanoparticle concentration. Additionally, ZnO nanoparticles may have caused bacterial cell membrane disruption and expulsion of cytoplasmic contents, which led to the death of the bacteria (Divyapriya *et al* 2014) [9].

Table 2: Antibacterial activity of zinc nanoparticles synthesis by the S. bularedii against Burkholderia cepacia

Concentration mg/ml	Inhibition zone rate (mm) isolation number									
	S1	**S2**	**S3**	**S4**	**S5**	**S6**	**S7**	**S8**	**S9**	**S10**
100	***5***	9	6	11	***10***	12	13	10	11	9
200	***8***	11	7	13	***13***	14	16	11	14	11
300	***11***	13	10	16	***18***	17	19	13	16	14

Antioxidant Activity of Biogenic ZnO NPs

The capacity of nanoparticles to scavenge DPPH free radicals was demonstrated in the study by examining the transformation of DPPH from its original (purple) hue to its current (yellow) color. With higher concentrations, ZnO NPs become more efficient at scavenging DPPH free radicals. The lowest inhibition was at a dosage of 0.12 mg/ml, whereas the maximum inhibition was at 1 mg/ml. Additionally, the study found that there were substantial variations in the amounts of ZnO NPs produced by S. bularedii (p 0.05). According to the Fig 9. The level of inhibition changes from one type of nanoparticle to another owing to an electron donation and DPPH acceptance (Kanipandian *et al* 2014; Bhakya *et al* 2015) [14, 3].

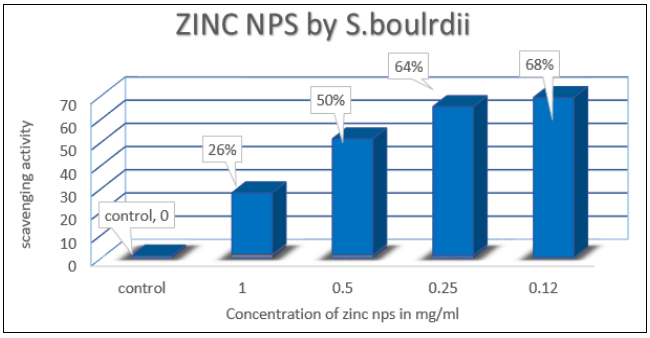

Fig 9: Antioxidant Activity of Biogenic Zinc NPs by DPPH assay synthesis by S. bularedii

References

1. Abdulhassan AJ. Effect of Silver and Titanium Nanoparticles Synthesized by Lactobacillus as Antimicrobial, Antioxidant and Some Physiological Parameters (Doctoral dissertation, Master Thesis. University of Kufa, Faculty of Science–Iraq), 2016.
2. Begum SJ, Pratibha S, Rawat JM, Venugopal D, Sahu P, Gowda A, Jaremko M. Recent Advances in Green Synthesis, Characterization and Applications of Bioactive Metallic Nanoparticles. Pharmaceuticals. 2022; 15(4):p455.
3. Bhakya S, Muthukrishnan S, Sukumaran M, Muthukumar M. Biogenic synthesis of iron nanoparticles and their antioxidant and antibacterial activity. Appl Nanosci. 2015; 6 (5):755-766.
4. Caroling G, Tiwari SK, Ranjitham AM, Suja R. Biosynthesis of Zinc nanoparticles using aqueous broccoli extract-characterization and study of antimicrobial, cytotoxic effects. Asian J Pharm Clin Res. 2013; 6 (4):165-172.
5. Chaudhari PR, Masurkar SA, Shidore VB, Kamble SP. Antimicrobial activity of extracellularly synthesized silver nanoparticles using Lactobacillus species obtained from VIZYLAC capsule. Journal of Applied Pharmaceutical Science, 2012, 25-29.
6. Dahiya D, Nigam PS. The Gut Microbiota Influenced by the Intake of Probiotics and Functional Foods with Prebiotics Can Sustain Wellness and Alleviate Certain Ailments like Gut-Inflammation and Colon-Cancer. Microorganisms. 2022; 10(3):p665.
7. Deepachitra R, Lakshmi RP, Sivaranjani K, Chandra JH, Sastry TP. Nanoparticles embedded biomaterials in wound treatment: A review. J. Chem. Pharm. Sci. 2015; 8:324-328.
8. Divya MJ, Sowmia C, Joona K, Dhanya KP. Synthesis of zinc oxide nanoparticle from Hibiscus rosa-sinensis leaf extract and investigation of its antimicrobial activity. Res. J. Pharm. Biol. Chem. 2013; 4(2):1137-1142.
9. Divyapriya S, Sowmia C, Sasikala S. Synthesis of zinc oxide nanoparticles and antimicrobial activity of Murraya Koenigii. World J. Pharm. Pharm. Sci. 2014; 3(12):1635-1645.
10. Dobrucka R, Długaszewska J. Biosynthesis and antibacterial activity of ZnO nanoparticles using Trifolium pratense flower extract. Saudi Journal of Biological Sciences. 2016; 23(4):517-523.
11. Durn N, Marcato PD, Durán M, Yadav A, Gade A. Mechanistic aspects in the biogenic synthesis of extracellular metal nanoparticles by peptides, bacteria, fungi, and plants. Applied microbiology and biotechnology. 2011; 90(5):1609-1624.
12. Goyal AK, Middha SK, Sen A. Evaluation of the DPPHradical scavenging activity, total phenols and antioxidant activities in Indian wild Bambusa vulgaris Vittata methanolic leaf extract. Journal of Natural Pharmaceuticals, 2010, 1(1).
13. Hicks CW, Selvarajah S, Mathioudakis N, Sherman RL, Hines KF, Black III JH, *et al*. Burden of infected diabetic foot ulcers on hospital admissions and costs. Annals of vascular surgery. 2016; 33:149-158.
14. Kanipandian N, Kannan S, Ramesh R, Subramanian P, Thirumurugan R. Characterization, antioxidant and cytotoxicity evaluation of green synthesized silver nanoparticles using Cleistanthus collinus extract as surface modifier. Materials Research Bulletin. 2014; 49:494-502.
15. Kaschner A, Haboeck U, Strassburg M, Strassburg M, Kaczmarczyk G, Hoffmann A, *et al*. Nitrogen-related local vibrational modes in ZnO: N. Applied Physics Letters. 2002; 80(11):1909-1911.
16. Laloy J, Minet V, Alpan L, Mullier F, Beken S, Toussaint O, *et al*. Impact of silver nanoparticles on haemolysis, platelet function and coagulation. Nanobiomedicine, 2014; 1:p4.
17. Loganathan S, Shivakumar MS, Karthi S, Nathan SS, Selvam K. Metal oxide nanoparticle synthesis (ZnO-NPs) of Knoxia sumatrensis (Retz.) DC. Aqueous leaf extract and It's evaluation of their antioxidant, anti-proliferative and larvicidal activities. Toxicology Reports. 2021; 8:64-72.
18. Mohd Yusof H, Rahman A, Mohamad R, Zaidan UH, Samsudin AA. Biosynthesis of zinc oxide nanoparticles by cell-biomass and supernatant of Lactobacillus plantarum TA4 and its antibacterial and biocompatibility properties. Scientific reports. 2020; 10(1):1-13.
19. Onyszko M, Markowska-Szczupak A, Rakoczy R, Paszkiewicz O, Janusz J, Gorgon-Kuza A, *et al*. The cellulose fibers functionalized with star-like zinc oxide nanoparticles with boosted antibacterial performance for hygienic products. Scientific Reports. 2022; 12(1):1-13.
20. Rajeshkumar S, Malarkodi C. *In vitro* antibacterial activity and mechanism of silver nanoparticles against foodborne pathogens. Bioinorganic chemistry and applications, 2014.
21. Ramesh P, Saravanan K, Manogar P, Johnson J, Vinoth E, Mayakannan M. Green synthesis and

characterization of biocompatible zinc oxide nanoparticles and evaluation of its antibacterial potential. Sensing and Bio-Sensing Research. 2021; 31:p100399.
22. Ranjan R, Chowdhary P, Kamra A. Community Acquired Burkholderia cepacia Bacteraemia Presenting as MODS in an Immunocompetent Individual: An Unusual Case. J Clin Diagn Res. 2017; 11(3).
23. Zhang S, Lin L, Huang X, Lu YG, Zheng DL, Feng Y. Antimicrobial Properties of Metal Nanoparticles and Their Oxide Materials and Their Applications in Oral Biology. Journal of Nanomaterials, 2022.
24. Shafaghat A. Synthesis and characterization of silver nanoparticles by phytosynthesis method and their biological activity. Synthesis and Reactivity in Inorganic, Metal-Organic, and Nano-Metal Chemistry. 2015; 45(3):381-387.
25. Shirley B, Jarochowska E. Chemical characterisation is rough: The impact of topography and measurement parameters on energy-dispersive X-ray spectroscopy in biominerals. Facies. 2022; 68(2):1-15.
26. Singh N, Armstrong DG, Lipsky BA. Preventing foot ulcers in patients with diabetes. J. Am. Med. Ass. 2005; 293:217-228. Doi: 10.1001/ jama.293.2.217
27. Stopnisek N, Zühlke D, Carlier A, Barberán A, Fierer N, *et al*. Molecular mechanisms underlying the close association between soil Burkholderia and fungi. ISME J. 2016; 10(1):p253.
28. Veve MP, Mercuro NJ, Sangiovanni RJ, Santarossa M, Patel N. Prevalence and Predictors of Pseudomonas aeruginosa among Hospitalized Patients with Diabetic Foot Infections. In Open Forum Infectious Diseases, 2022.
29. Xu Y, Buss EA, Boucias DG. Culturing and Characterization of Gut Symbiont Burkholderia spp. from the Southern Chinch Bug, Blissus insularis (Hemiptera: Blissidae), 2016.
30. Yallappa S, Manjanna J, Sindhe MA, Satyanarayan ND, Pramod SN, Nagaraja K. Microwave assisted rapid synthesis and biological evaluation of stable copper nanoparticles using T. arjuna bark extract. Spectrochimica Acta Part A: Molecular and Biomolecular Spectroscopy. 2013; 110:108-115.
31. Zhang S, Lin L, Huang X, Lu YG, Zheng DL, Feng Y. Antimicrobial Properties of Metal Nanoparticles and Their Oxide Materials and Their Applications in Oral Biology. Journal of Nanomaterials, 2022.